Mohammed Mahmood, Ahmed Elamin, Walid Tizani, (2020), Ultimate Strength and Fracture Sequence of Bolted Connections to Thin-Walled Carbon Steel, Journal of Structures, 23 Elsevier, 23(2020) 646–659, https://doi.org/10.1016/j.istruc.2019.11.011

Ultimate Strength and Fracture Sequence of Bolted Connections to Thin-Walled Carbon Steel

Mohammed Mahmood[1], Ahmed Elamin[2] and Walid Tizani[3]

[1]Department of Civil Engineering, University of Diyala, Iraq

[2]Department of Civil Engineering, The University of Nottingham Ningbo China

[3]Department of Civil Engineering, The University of Nottingham, UK

Abstract

Recent experimental studies on single shear bolted connections to thin-walled carbon steel indicate the need for parametric analysis to understand the behaviour of the connection. In this paper, finite element analysis was performed to investigate the ultimate behaviour and failure sequence of these connections. A parametric analysis was performed to investigate the effect of plate thickness, end distance and curling displacement on the connection behaviour. Five possible modes of failure were identified and analytical models for estimating the connection strength for these modes were proposed. Within the range of the validity of the study, the end distance was the most influential parameter, but the strength improvement becomes negligible at edge distance of 42mm for plate thickness less than or equal to 3.5mm and 48mm for plate thickness greater than 3.5mm. Therefore, it is recommended to limit the maximum end distance to 50mm. The curling displacement is found to affect the stress distribution in the plate as it could reduce the connection strength by 12%. It is considered as a sign of failure only when it reaches 0.5mm before the ultimate strength of the connection is reached. The proposed models are more accurate in predicting the connection ultimate strength when compared to EC3, AISI and AISC predictions.

Keywords: *Bolted connections; Thin-walled Carbon steel; Single shear bolt; Fracture sequence.*

1. INTRODUCTION

For practical reasons, bolted joints are widely used in steel structures. They allow for a quick and easy assembly of structural elements and can transfer bending, shear and axial forces [1]. The construction industry saw an increase in the use of thin-walled (light gauge) steel elements as structural members in recent years. However, reliable connection design information for these sections are not available. Such information, in addition to economical and versatile properties of

thin-walled steel, can make these elements more attractive over other forms of construction. Early example of research into the area of thin-walled connection is the study of Winter [2], which focused mainly on bolted connections. Kim and Yura in 1999 conducted an experimental study on the effect of end distance on the bearing strength in one and two lap connections. It was reported that a large end distance results in higher deformation at the ultimate strength [3]. Topkaya in 2004 [4] proposed equations for calculating block shear load capacity for steel tension members based on finite element analysis results. Kim and Kuwamura in 2007 [5] performed finite element analysis to investigate the behaviour of thin-walled single shear stainless steel bolted connections. The out of plane displacement in the direction of the plate thickness which occurs at the end of the connection plate (curling) was reported as an influential parameter on the ultimate strength of the connection. A parametric study using finite element was performed by Kim et al. [6] to investigate the ultimate strength and curling behaviour of single shear bolted connections. It was confirmed that the effect of curling should be considered in estimating the connection strength and accordingly a revised design formula was suggested. Teh and Clements [7] performed experimental study to examine the mechanism of block shear failure in bolted connections in G450 steel sheets. The study defined shear lag factor and proposed more accurate rational equation to predict the connection strength. Clements and Teh [8] used finite element analysis to examine the behaviour of bolted connection in steel sheets. The shear failure planes were identified at midway between the gross and the net shear planes and termed as active shear plane. Kim and Lim [9] employed finite element analysis to predict the ultimate strength, fracture mode and curling in austenitic stainless steel single shear bolted connections. It was confirmed that the occurrence of curling displacement reduces the ultimate strength and changes the fracture patterns. An extensive experimental study in addition to finite element analysis were conducted by Kim et al. [10, 11] to investigate the fracture mechanism and the curling behaviour in single shear bolted connection in thin-walled carbon steel. The main variables of the tests were the plate thickness and the end distance. Curling was reported to occur in specimens with large end distance, which was a companied by a reduction in the ultimate strength of the connection.

Figure 1: Light steel thin-walled structures [12]

The evidence presented in the literature suggests that the available design equations for thin-walled carbon steel single shear bolted connections are not adequately simulating the failure modes. Therefore, there is a need to device more precise equations that can simulate the real behaviour of the connection and provide reliable estimation to the connection strength.

Hence, the aim of this research is to investigate the ultimate strength and fracture sequence of single shear bolted connections to thin-walled carbon steel. Parametric finite element analysis were performed to provide adequate information which could be used to devise analytical models that can be used in the design of this type of connection considering both safety and economy.

2. FINITE ELEMENT MODELLING

The Finite Element (FE) package ABAQUS 6.11 [13] was used to simulate the behaviour of thin-walled carbon steel single shear bolted connections. The model consists of three components: test plate, pulling plate and bolts (as shown in Figure 2). Three dimensional continuum reduced integration element (C3D8R) [13] were selected to simulate the three components of the model. This element is suitable for simulating highly nonlinear behaviour including contact and geometrical nonlinearities. The geometrical and materials properties of the model are identical to the specimens tested by Kim et al. [10]. Figure 3 and Table 1 present the geometrical and materials properties of the model components. The specimen name describes its geometrical properties. For example, T1.5E24 denotes that the thickness of the test plate is 1.5mm and the end distance (e_1) is 24mm. The exact geometrical properties were used to generate the model. The material properties listed in Table 1 were converted to true values and then fed to the FE model. The bolts and the pulling plate were simulated as elastic materials, whereas, the test plate was modelled as elastic plastic material using bilinear stress-strain relation [14].

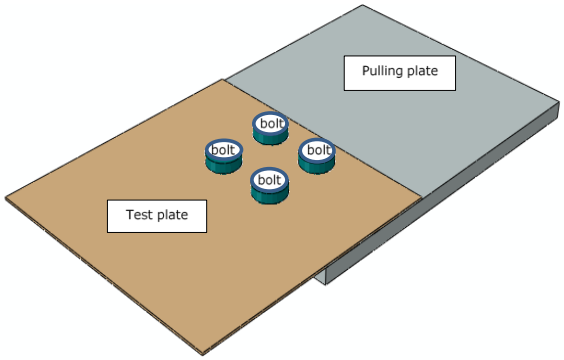

Figure 2: FE model components

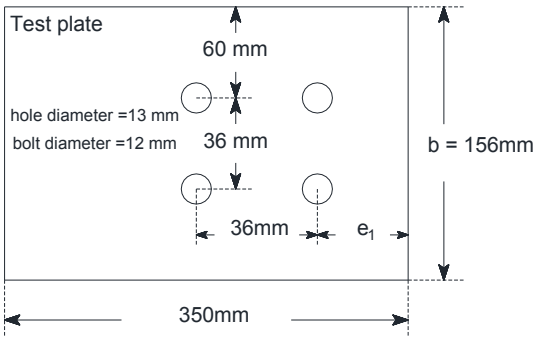

a. Test plate

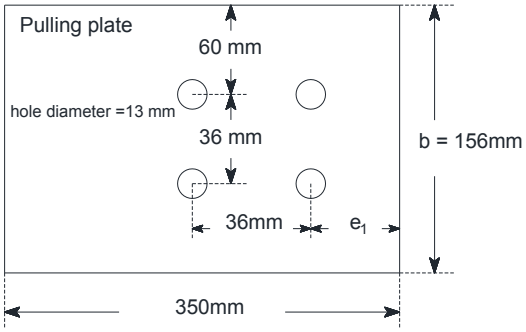

b. Pulling plate (thickness=10mm)

Figure 3: Model geometry of specimens tested by Kim et al. [10]

Table 1: Material properties of specimens tested by Kim et al. [10]

Specimens	Young's modulus E (GPa)	Yield strength f_y (MPa)	Ultimate strength f_u (MPa)	Elongation %
T1.5E12, T1.5E18, T1.5E24 & T1.5E36	201	344	434	34.67
T3.0E24, T3.0E30, T3.0E36, T3.0E48 & T3.0E60	213	345	498	32.00
T6.0E36, T6.0E48, T6.0E48, T6.0E54 & T6.0E60	193	222	334	49.90

Surface to surface contact algorithm was used to simulate the contact between the different parts of the model. Both hard and tangential contacts existed in the model. The friction coefficient was considered equal to 0.45 [15]. To avoid stress concentration at the test plate, the support boundary condition was distributed over an area equal to b×20mm, where b is the width of the test plate, Figure 4. Mesh sensitivity analysis was performed to identify the optimum element size and it was found that mesh size 0.5t (t is the test plate thickness) is suitable to use at the area close to the holes and the rest of the model could be meshed using coarser element (Figure 5).

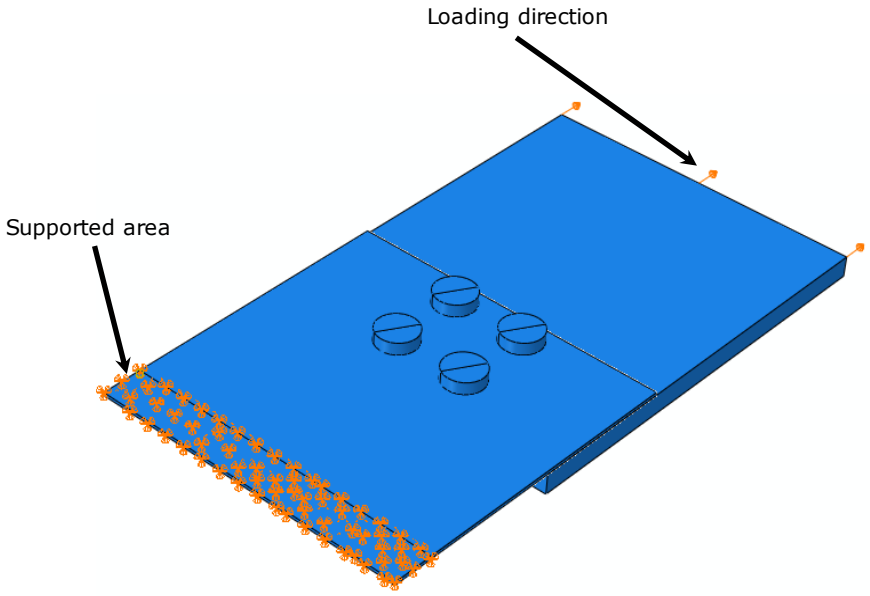

Figure 4: Model boundary conditions

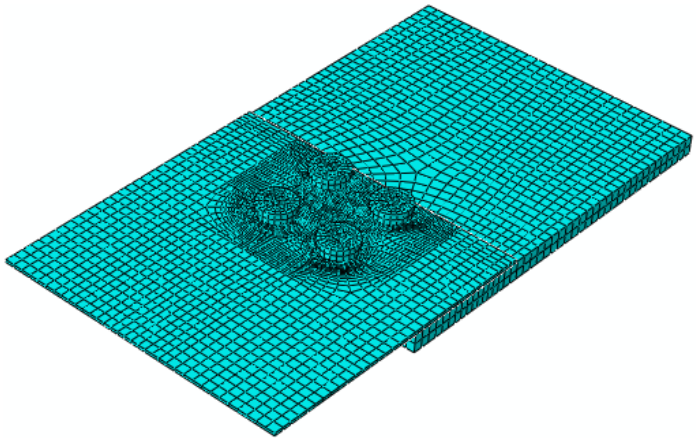

Figure 5: Model mesh

3. FE MODEL VALIDATION

In order to verify the accuracy of the numerical model, its results were compared with experimental data and observations from the literature. Figure 6 shows a comparison between the FE results and experimental data reported by Kim et al. [10]. The general pattern of the FE curves shows good correlation with the experimental data.

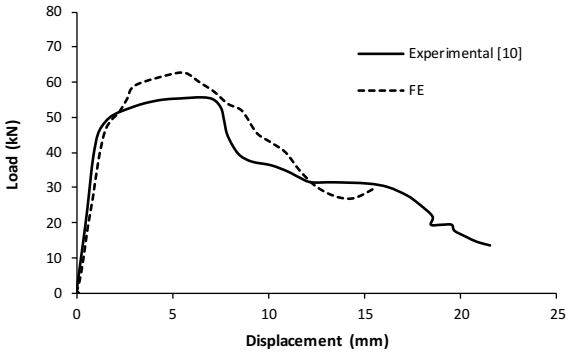

a. T1.5E12

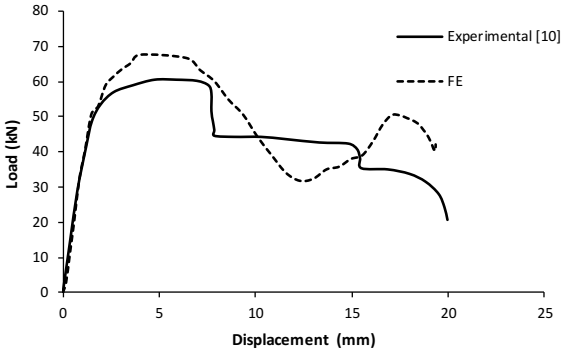

b. T1.5E18

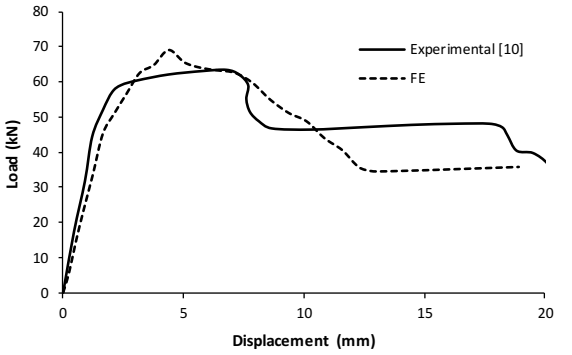

c. T1.5E24

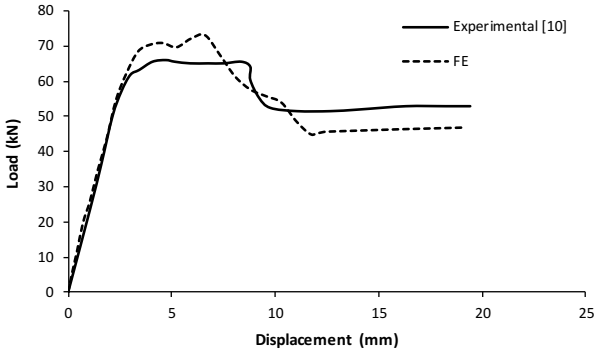

d. T1.5E36

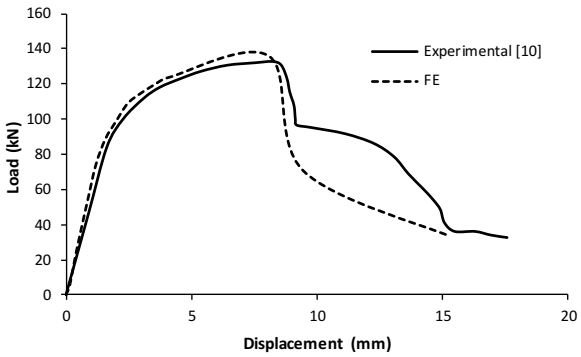

e. T3.0E24

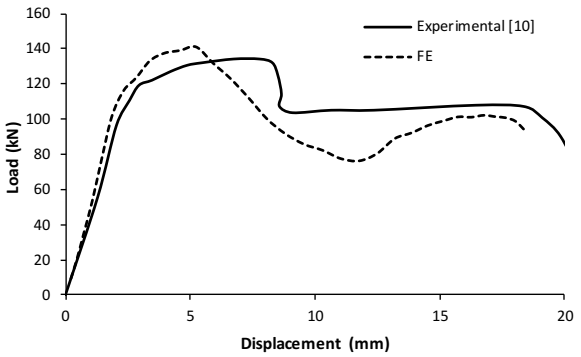

f. T3.0E30

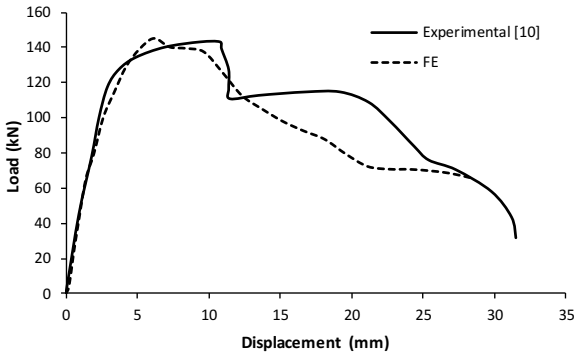

g. T3.0E36

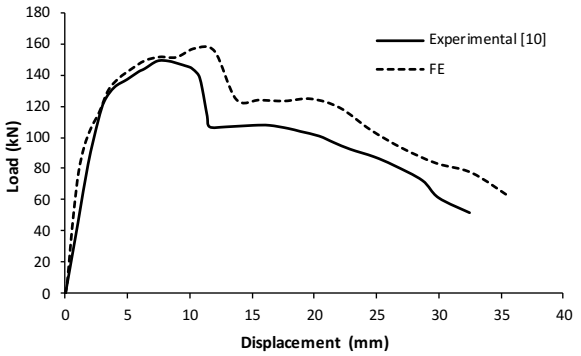

h. T3.0E48

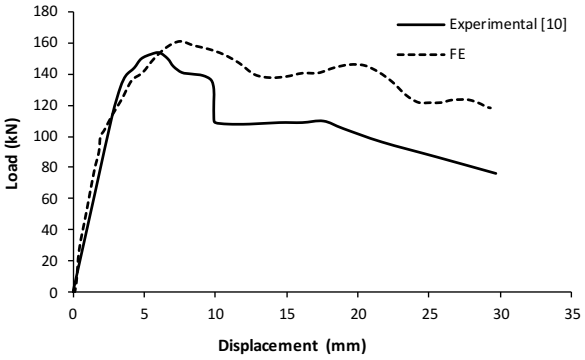

i. T3.0E60

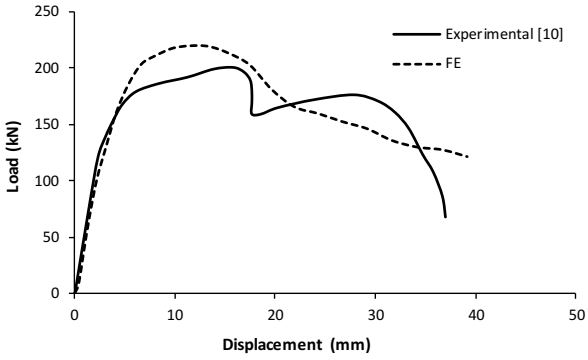

j. T6.0E36

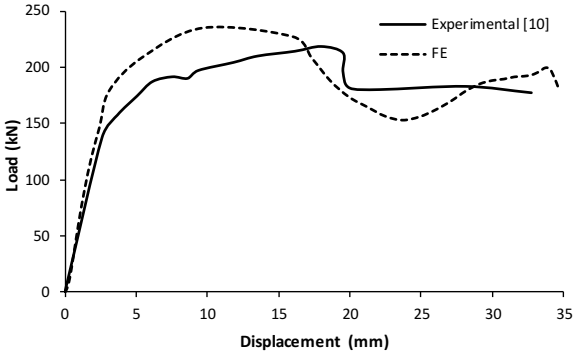

k. T6.0E48

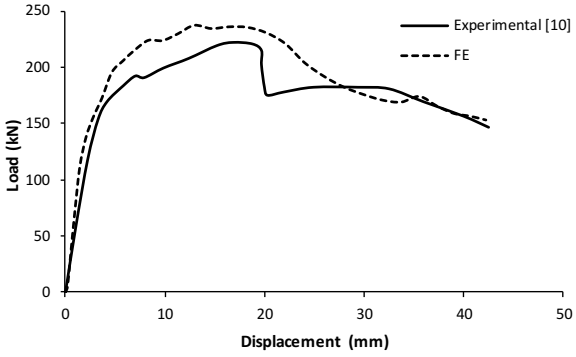

l. T6.0E54

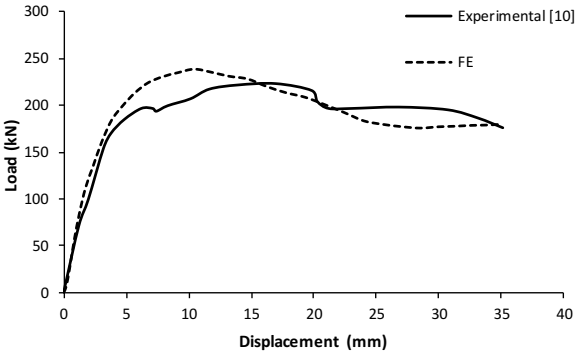

m. T6.0E60

Figure 6: Load displacement curves FE Vs. experimental data from Kim et al [10].

Table 2 summarises a comparison between the ultimate strength (P_u) and curling displacement (Δ_c) from FE analysis and experimental data [10]. The maximum mean value of ratio of finite element ultimate strength to the experimental ultimate strength (P_{uf}/P_{ue}) and corresponding coefficient of variation are 1.08 and 0.037 respectively. Figure 7 shows the ability of the FE model to capture the failure mode accurately. This indicates that the FE model can accurately simulate the behaviour of the connection.

Table 2: Ultimate strength and curling displacement FE Vs. experimental from Kim et al [10]

Specimens	Ultimate strength P_u			Curling displacement at P_u		
	Exp. P_{ue} kN	FE P_{uf} kN	P_{uf}/P_{ue}	Exp. Δ_{ce} mm	FE Δ_{cf} mm	Δ_{cf}/Δ_{ce}
T1.5E12	54.68	62.58	1.14	---	---	---
T1.5E18	60.50	67.53	1.12	---	---	---
T1.5E24	61.28	69.08	1.13	---	---	---
T1.5E36	66.12	73.10	1.11	3.22	3.15	0.98
T3.0E24	131.38	138.40	1.05	---	---	---
T3.0E30	134.52	141.10	1.05	---	---	---
T3.0E36	142.92	145.40	1.02	3.12	2.79	0.89
T3.0E48	148.63	157.29	1.06	5.46	4.71	0.86
T3.0E60	153.57	161.07	1.05	0.55	0.50	0.91
T6.0E36	201.00	220.06	1.09	0.87	0.81	0.93
T6.0E48	215.54	235.12	1.09	1.22	1.13	0.93
T6.0E54	220.50	237.26	1.08	1.08	0.98	0.91
T6.0E60	222.40	238.18	1.07	0.95	0.85	0.89
	Mean		1.08			0.91
	Standard deviation		0.036			0.034
	Coefficient of variation		0.034			0.037

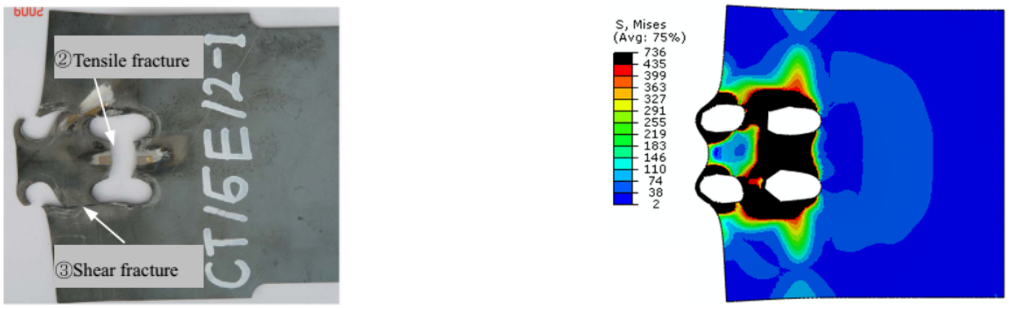

T1.5E12

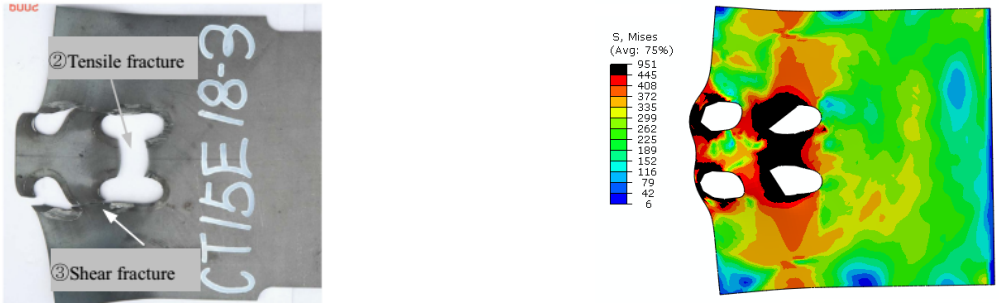

T1.5E18

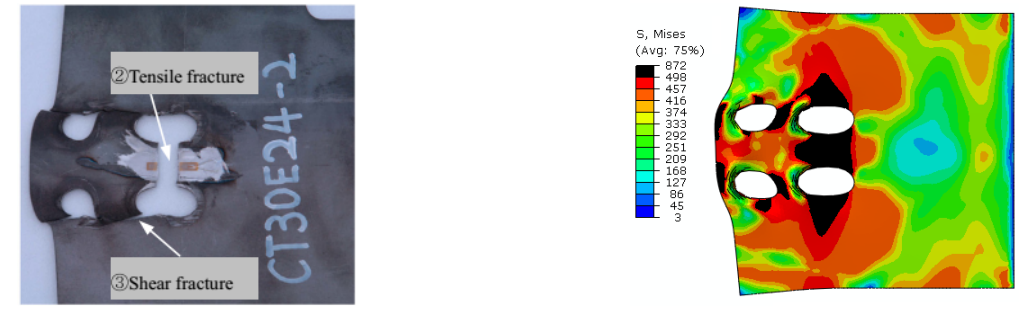

T30E24

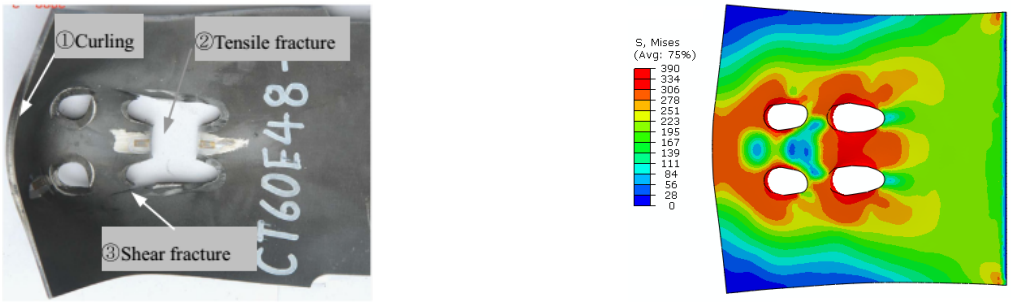

T60E48

Figure 7: Failure modes FE versus experimental from Kim et al [10]

4. FE ANALYSIS AND PARAMETRIC STUDY

The parametric study investigates the effect of plate thickness, end distance e_1 and the constraint of curling displacement. The other parameters are kept constant for all specimens. The bolt gauge and pitch distances are equal to 36mm. The bolt diameter is 12mm and the hole diameter is 13mm. The edge distance e_2 is equal to 60mm. The Young modulus of elasticity is 201GPa, the yield strength is 344MP, the ultimate strength is 434MPaa and the fracture elongation is 34.67%.

4.1 Failure Criteria and Curling

Experimental evidence, [10], confirmed that the ultimate strength in thin-walled carbon steel is governed by the fracture and the curling of the steel plate. In previous numerical analysis [5, 14, 16, 17], it was stated that the fracture initiates when the direct stress or strain in the steel plate approaches its ultimate values. Hence, bolted joints reach their ultimate limit state (ultimate strength) when the stress or strain becomes greater or equal to the true values. Accordingly, the following assumption is adopted to predict the failure criteria:

$$\frac{\sigma}{\sigma_{t\,max}} \geq 1.0 \qquad \rightarrow \text{ fracture exists in the plate}$$

where σ is the direct stress and $\sigma_{t\,max}$ is the maximum stress (ultimate stress).

The FE results showed that there are five possible modes of failure that could govern the behaviour of the bolted connections in thin-walled carbon steel:

- **Mode 1 (**Figure 8, a)**:** Tensile fracture of the plate between the holes transvers to the loading direction, shear fracture between the holes parallel to the loading direction and bending fracture at the end distance parallel to the loading direction.
- **Mode 2 (**Figure 8, b)**:** Tensile fracture of the plate between the holes transvers to the loading direction, shear fracture between the holes parallel to the loading direction and bending yielding at the end distance parallel to the loading direction.
- **Mode 3 (**Figure 8, c)**:** Tensile yielding in the plate between the holes transvers to the loading direction, shear yielding between the holes parallel to the loading direction and bending yielding in the end distance parallel to the loading direction.
- **Mode 4 (**Figure 8, d and f)**:** Curling, tensile yielding in the plate between the holes transvers to the loading direction and bending yielding in the end distance parallel to the loading direction. It is clear that the curling prevents the shear yielding between the holes parallel to the loading direction.
- **Mode 5 (**Figure 8, e)**:** Gross yielding across the width of the plate transvers to the loading direction.

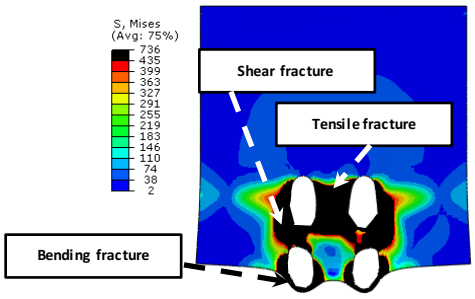

T1.5E12

a. Mode 1

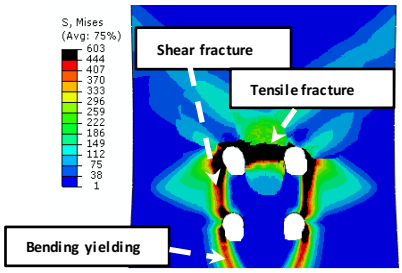

T2.0E18

b. Mode 2

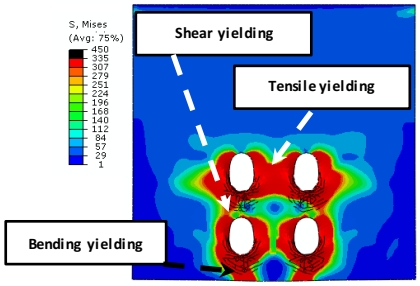

T3.5E24

c. Mode 3

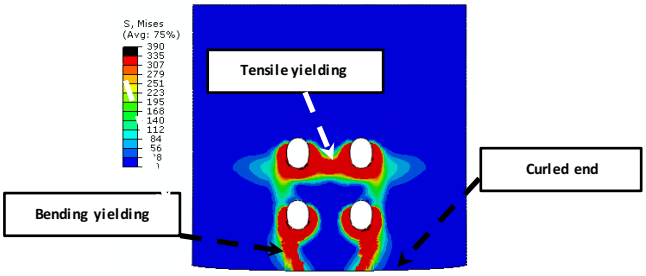

T5.5E30

d. Mode 4

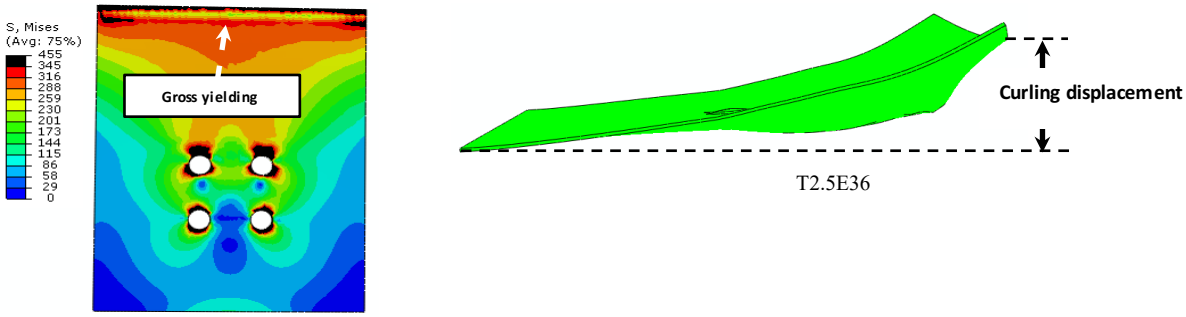

e. Mode 5 f. Curling

Figure 8: Failure modes

4.2 Influence of end distance

Figure 9 shows the effect of end distance on the ultimate strength of the bolted connections in thin-walled carbon steel. The end distance was varied from 12mm to 60mm for six plates with thickness of 1.5, 2.5, 3.5, 4.5, 5.5, and 6.5 millimetres. The results present clear improvement in the connection strength with the increase of the end distance. However, the improvement becomes negligible after edge distance of 42mm for plate thickness less than or equal to 3.5mm and 48mm for plate thickness greater than 3.5mm. This could be attributed to the changing of failure mode to gross yielding in the plate transvers to the loading direction (Mode 5) at these end distances (Figure 10). Since Mode 5 is gross yielding mechanism and the connection strength does not depend on the end distance. Therefore, it is recommended that the maximum end distance measured parallel to the loading direction to be equal to 50 millimetres.

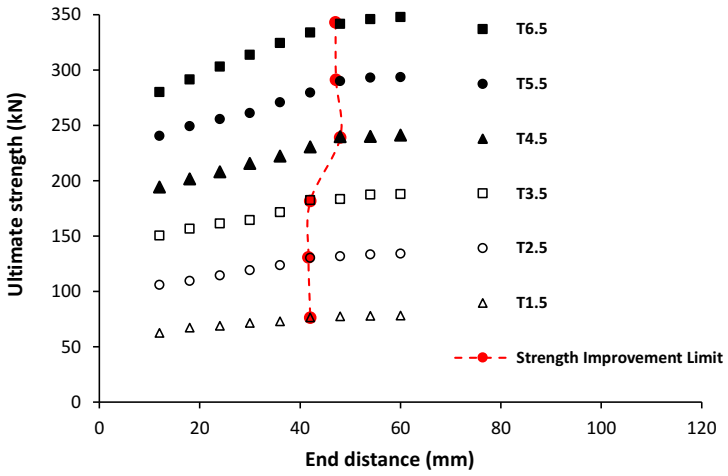

Figure 9: Effect of end distance on ultimate strength

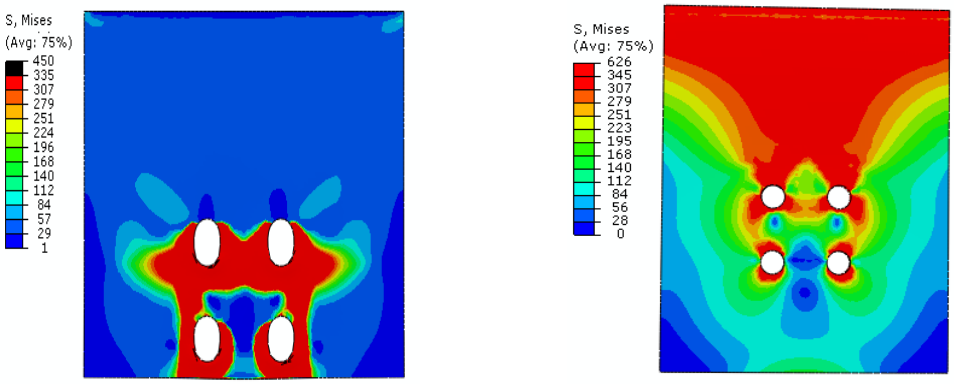

a. T6.5E12 b. T6.5E60

Figure 10: Influence of edge distance on failure mode

4.3 Influence of curling

Curling could affect the connection performance in different manners. It could improve the buckling capacity of wide flange sections [18] or reduce the connection capacity [10]. A limit of 0.3mm curling displacement was suggested by Kim et al. [6] as a failure criterion for single shear bolted connections in cold formed austenitic stainless steel. To investigate the effect of curling, the specimens that failed by curling (Mode 4) were reanalysed with a constraint against curling. The constraint was added to the face of the specimens along the end distance to prevent any out of plane displacement in the direction of the plate thickness. The letter S was added to the end of the name of the specimens to indicate this constraint. For example, T1.5E30 is free to curl specimen, whereas T1.5E30S is constrained against curling specimen. Figure 11 shows that the existence of curling could limit the connection strength. The maximum reduction in the connection strength due curling is equal to 12% (Table 3). For the curled specimens, the load displacement relation shows sharp drop in the strength after reaching the ultimate capacity. However, the drop in the strength was softer for constrained specimens. Also it was found that the presence of curling could change the strain distribution around the bolt holes (Figure 12). Table 4 presents that Mode4 (curling mode) exists only when the curling displacement at P_u is larger than 0.5mm. Therefore, the curling displacement can be considered as a failure criterion only when it exceeds 0.5mm before the presence of any of the failure modes described above.

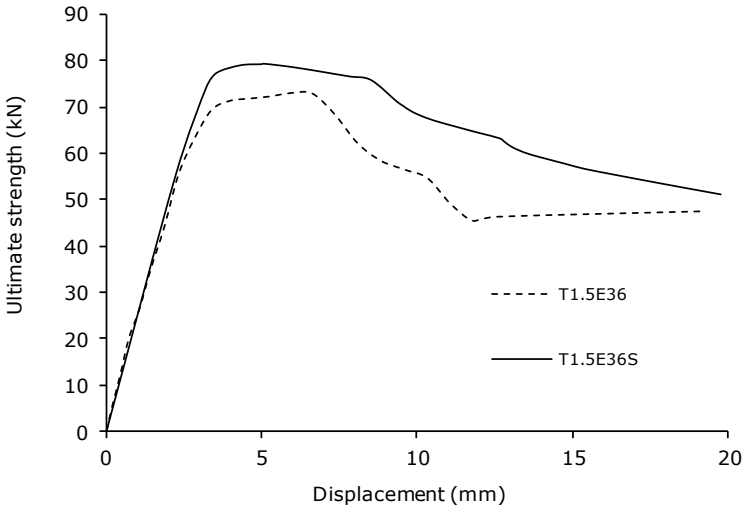

a. T1.5E36 vs. T1.5E36S

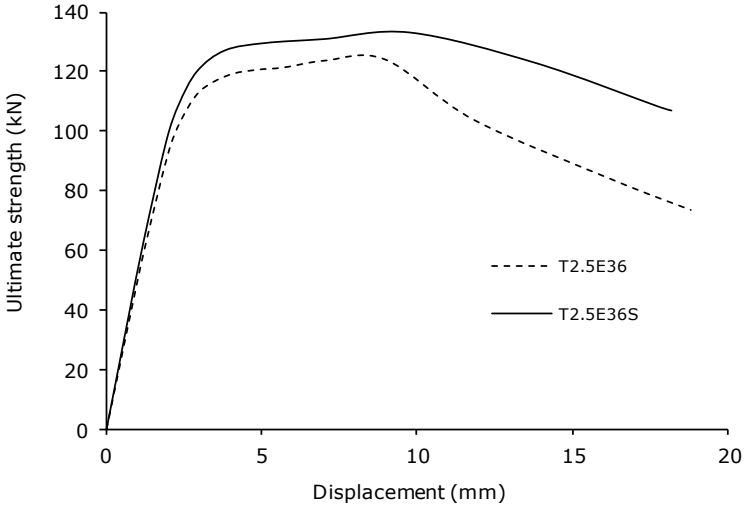

b. T2.5E30 vs. T2.5E30S

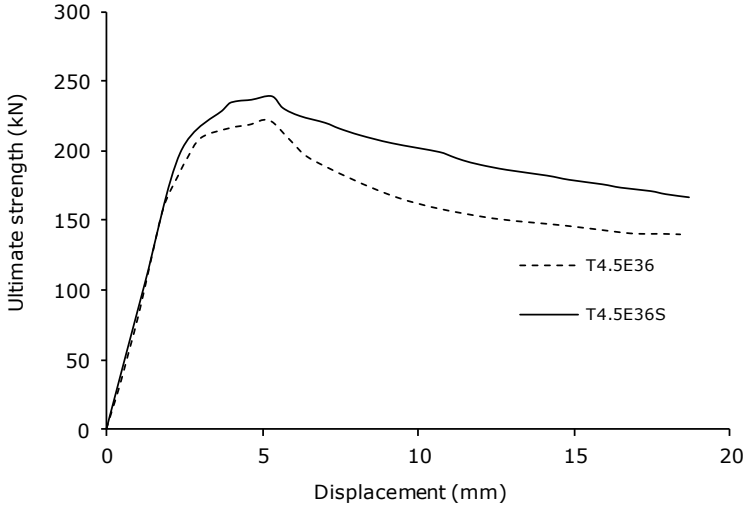

c. T4.5E36 vs. T4.5E36S

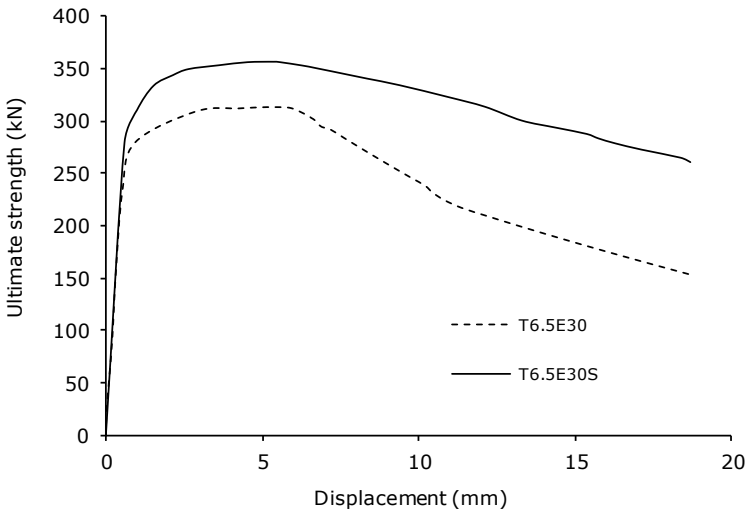

d. T6.5E30 vs. T6.5E30S

Figure 11: Influence of curling on the connection behaviour

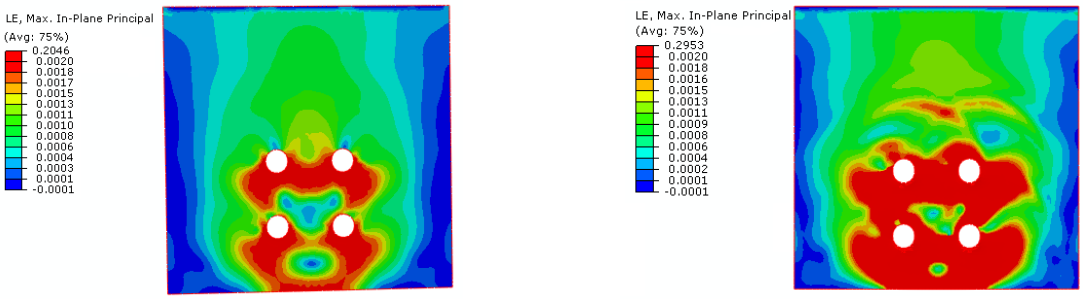

a. T5.5E30 b. T5.5E30S

Figure 12: Influence of curling on strain distribution

Table 3: The ultimate strength of curled and uncurled specimens

Curled Specimens	$P_{u\ curled}$	Uncurled Specimens	$P_{u\ uncurled}$	$P_{u\ curled}/P_{u\ uncurled}$
T1.5E30	71.622	T1.5E30S	78.712	0.91
T1.5E36	73.102	T1.5E36S	79.325	0.92
T2.0E30	92.561	T2.0E30S	104.587	0.89
T2.0E36	98.987	T2.0E36S	106.358	0.93
T2.5E30	119.359	T2.5E30S	131.618	0.91
T2.5E36	123.767	T2.5E36S	133.122	0.93
T3.0E30	143.625	T3.0E30S	158.125	0.91
T3.0E36	152.014	T3.0E36S	159.512	0.95
T3.5E30	164.612	T3.5E30S	184.254	0.89
T3.5E36	171.630	T3.5E36S	183.614	0.93
T4.0E30	189.222	T4.0E30S	214.987	0.88

T4.0E36	198.954	T4.0E36S	213.554	0.93
T4.0E42	212.106	T4.0E42S	216.546	0.98
T4.5E30	215.723	T4.5E30S	238.156	0.91
T4.5E36	222.354	T4.5E36S	235.751	0.94
T4.5E42	230.789	T4.5E42S	244.381	0.94
T5.0E30	238.687	T5.0E30S	268.147	0.89
T5.0E36	248.729	T5.0E36S	266.584	0.93
T5.0E42	257.798	T5.0E42S	270.541	0.95
T5.5E30	261.189	T5.5E30S	294.872	0.89
T5.5E36	271.051	T5.5E36S	296.175	0.92
T5.5E42	279.629	T5.5E42S	296.548	0.94
T6.0E30	285.876	T6.0E30S	322.144	0.89
T6.0E36	298.658	T6.0E36S	322.555	0.93
T6.0E42	315.586	T6.0E42S	323.546	0.98
T6.5E30	313.737	T6.5E30S	355.996	0.88
T6.5E36	324.402	T6.5E36S	350.248	0.93
T6.5E42	333.942	T6.5E42S	351.698	0.95

Table 4: Curling displacement

Specimen	Curling displacement at P_u (mm)	Failure mode	Specimen	Curling displacement at P_u (mm)	Failure mode	Specimen	Curling displacement at P_u (mm)	Failure mode
T1.5E12	0.146	Mode 1	T3.0E48	0.382	Mode 5	**T5.0E30**	**0.662**	**Mode 4**
T1.5E18	0.338	Mode 2	T3.0E54	0.304	Mode 5	**T5.0E36**	**0.733**	**Mode 4**
T1.5E24	0.434	Mode 3	T3.0E60	0.107	Mode 5	**T5.0E42**	**0.683**	**Mode 4**
T1.5E30	**0.532**	**Mode 4**	T3.5E12	0.154	Mode 1	T5.0E48	0.456	Mode 5
T1.5E36	**0.543**	**Mode 4**	T3.5E18	0.354	Mode 2	T5.0E54	0.418	Mode 5
T1.5E42	0.434	Mode 5	T3.5E24	0.456	Mode 3	T5.0E60	0.147	Mode 5
T1.5E48	0.389	Mode 5	**T3.5E30**	**0.559**	**Mode 4**	T5.5E12	0.184	Mode 1
T1.5E54	0.310	Mode 5	**T3.5E36**	**0.570**	**Mode 4**	T5.5E18	0.425	Mode 2
T1.5E60	0.109	Mode 5	T3.5E42	0.456	Mode 5	T5.5E24	0.442	Mode 3
T2.0E12	0.145	Mode 1	T3.5E48	0.408	Mode 5	**T5.5E30**	**0.617**	**Mode 4**
T2.0E18	0.334	Mode 2	T3.5E54	0.325	Mode 5	**T5.5E36**	**0.684**	**Mode 4**
T2.0E24	0.430	Mode 3	T3.5E60	0.114	Mode 5	**T5.5E42**	**0.637**	**Mode 4**
T2.0E30	**0.527**	**Mode 4**	T4.0E12	0.165	Mode 1	T5.5E48	0.425	Mode 5
T2.0E36	**0.537**	**Mode 4**	T4.0E18	0.380	Mode 2	T5.5E54	0.390	Mode 5
T2.0E42	0.430	Mode 5	T4.0E24	0.488	Mode 3	T5.5E60	0.137	Mode 5
T2.0E48	0.385	Mode 5	**T4.0E30**	**0.599**	**Mode 4**	T6.0E12	0.169	Mode 1
T2.0E54	0.306	Mode 5	**T4.0E36**	**0.611**	**Mode 4**	T6.0E18	0.391	Mode 2
T2.0E60	0.108	Mode 5	**T4.0E42**	**0.585**	**Mode 4**	T6.0E24	0.406	Mode 3
T2.5E12	0.148	Mode 1	T4.0E48	0.438	Mode 5	**T6.0E30**	**0.567**	**Mode 4**
T2.5E18	0.342	Mode 2	T4.0E54	0.348	Mode 5	**T6.0E36**	**0.628**	**Mode 4**

Specimen	Curling displacement at P_u (mm)	Failure mode	Specimen	Curling displacement at P_u (mm)	Failure mode	Specimen	Curling displacement at P_u (mm)	Failure mode
T2.5E24	0.439	Mode 3	T4.0E60	0.123	Mode 5	**T6.0E42**	**0.585**	**Mode 4**
T2.5E30	**0.539**	**Mode 4**	T4.5E12	0.175	Mode 1	T6.0E48	0.391	Mode 5
T2.5E36	**0.550**	**Mode 4**	T4.5E18	0.405	Mode 2	T6.0E54	0.358	Mode 5
T2.5E42	0.439	Mode 5	T4.5E24	0.467	Mode 3	T6.0E60	0.126	Mode 5
T2.5E48	0.394	Mode 5	**T4.5E30**	**0.638**	**Mode 4**	T6.5E12	0.161	Mode 1
T2.5E54	0.313	Mode 5	**T4.5E36**	**0.651**	**Mode 4**	T6.5E18	0.371	Mode 2
T2.5E60	0.110	Mode 5	**T4.5E42**	**0.623**	**Mode 4**	T6.5E24	0.386	Mode 3
T3.0E12	0.144	Mode 1	T4.5E48	0.467	Mode 5	**T6.5E30**	**0.539**	**Mode 4**
T3.0E18	0.331	Mode 2	T4.5E54	0.371	Mode 5	**T6.5E36**	**0.597**	**Mode 4**
T3.0E24	0.426	Mode 3	T4.5E60	0.131	Mode 5	**T6.5E42**	**0.556**	**Mode 4**
T3.0E30	**0.522**	**Mode 4**	T5.0E12	0.197	Mode 1	T6.5E48	0.371	Mode 5
T3.0E36	**0.533**	**Mode 4**	T5.0E18	0.456	Mode 2	T6.5E54	0.341	Mode 5
T3.0E42	0.426	Mode 5	T5.0E24	0.474	Mode 3	T6.5E60	0.120	Mode 5

5. ESTIMATION OF ULTIMATE STRENGTH

The design standards for steel structures such as Euro Code (EC3) [19, 20], American Iron and Steel Institute (AISI) specification[21], American Institute of Steel Construction (AISC) manual [22] provide design rules for calculating the strength of shear bolted connections. EC3 describes the ultimate strength of the connection by tensile fracture of net section area (A_{nt}) and shear yielding of net section area (A_{ns}).

$$P_u = A_{nt}\ F_u + \frac{A_{ns}\ F_y}{\sqrt{3}} \quad (1)$$

AISI [21] and AISC [22] define the ultimate strength of the connection by the minimum of equations 2 and 3

$$P_u = A_{nt}\ F_u + 0.6\,A_{gs}\ F_y \quad (2)$$

$$P_u = A_{nt}\ F_u + 0.6\,A_{ns}\ F_u \quad (3)$$

Where, A_{gs} is the gross area subject to shear.

Teh et al. in 2011 [23] suggested equation (4) for calculating the block shear fracture strength of bolted connections in cold-reduced steel sheets (G450). The equation considers both of net section tensile fracture and active shear fracture.

$$P_u = A_{nt}\ F_u(0.9 + 0.1\,\frac{d}{g}) + 0.6\,A_{av}\ F_y \quad (4)$$

Where, A_{av} is the active gross area subject to shear = $2(\ L_{gv} - \left(\frac{n_1 - 1}{2} + 0.25\right) \times \emptyset) \times t$, L_{gv} is the length of gross area subjected to shear and n_1 is number of bolts in the loading direction.

Equations (1-4) consider only the shear and tensile failure criteria. The evidence presented in section 5 confirmed that bending and curling should be considered in addition to shear and tensile failure criteria. Therefore, there is a need to device more precise equations that can simulate the real behaviour of the connection and provide reliable estimation to the connection strength. The failure modes which are presented in section 5 can be idealized as shown in Figure 13. The ultimate strength of single shear bolted connection in thin-walled carbon steel can be calculated as follows:

Mode 1: (Figure 13,a)

$$P_u = P_{ut} + P_{us} + P_{ub} \quad (5)$$

Where,

P_u : the ultimate strength of single shear bolted connection in thin-walled carbon steel

P_{ut} : the net tensile fracture strength

P_{us} : the net shear fracture strength

P_{ub} : the bending fracture strength

$$P_{ut} = A_{nt}\ F_u \quad (6)$$

$$P_{us} = A_{ns}\ 0.6\ F_u \quad (7)$$

Kuwamura et al. (cited in [6]) suggested equations (7-9) to calculate the ultimate strength of bending fracture (P_{ub}).

When, $g \geq 2e_o$

$$P_{ub} = n_t \frac{4\ t\ e_o^2}{d}\ F_u\ , \qquad 2e_o \leq d \quad (8)$$

$$P_{ub} = n_t \frac{4\ t\ e_o^2}{4e_o - d}\ F_u\ , \qquad 2e_o > d \quad (9)$$

When, $g < 2e_o$

$$P_{ub} = n_t \frac{t}{2}\left[e_o + \left(1 + \frac{g + \emptyset}{4e_o}\right) g_o\right] F_u \quad (10)$$

Where,

A_{nt} : net tensile area = $(g - \emptyset)\ t$

g: bolt gauge distance

$\emptyset$: hole diameter

t : steel plate thickness

F_u: the ultimate tensile strength for steel plate

A_{ns}: net shear area = $(p - \emptyset)\ t$

p: bolt pitch distance

$$e_o = e_1 - \frac{\emptyset}{2}$$

$$g_o = g - \emptyset$$

n_t: total number of bolts

d : bolt diameter

Mode 2: (Figure 13, b)

$$P_u = P_{ut} + P_{us} + P_{yb} \quad (11)$$

Where, P_{yb} is the bending yielding strength and it can be calculated by replacing the ultimate tensile strength F_u by the yielding tensile strength F_y in equations (8-10).

Mode 3: (Figure 13, c)

$$P_u = P_{yt} + P_{ys} + P_{yb} \quad (12)$$

$$P_{yt} = A_{nt}\ F_y \quad (13)$$

$$P_{ys} = A_{ns}\ 0.6\ F_y \quad (14)$$

Where,

P_{yt}: net tensile yielding strength

P_{ys}: net shear yielding strength

Mode 4: Curling mode (Figure 13, d)

$$P_u = P_{yt} + P_{yb} \quad (15)$$

Mode 5: (Figure 13, e)

$$P_u = b\ t\ F_y \quad (16)$$

Where,

b : width of the steel plate

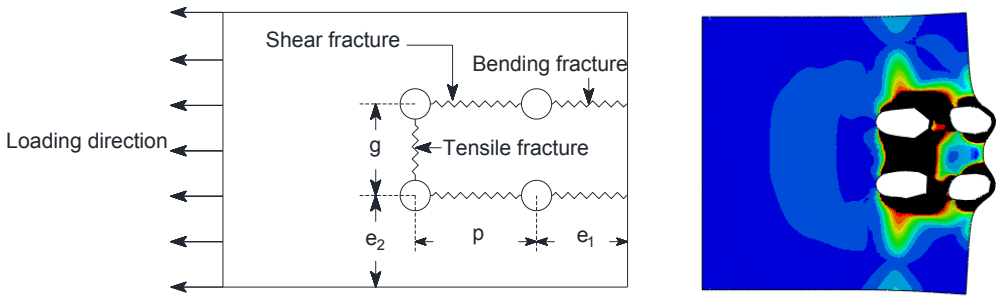

a. Mode 1

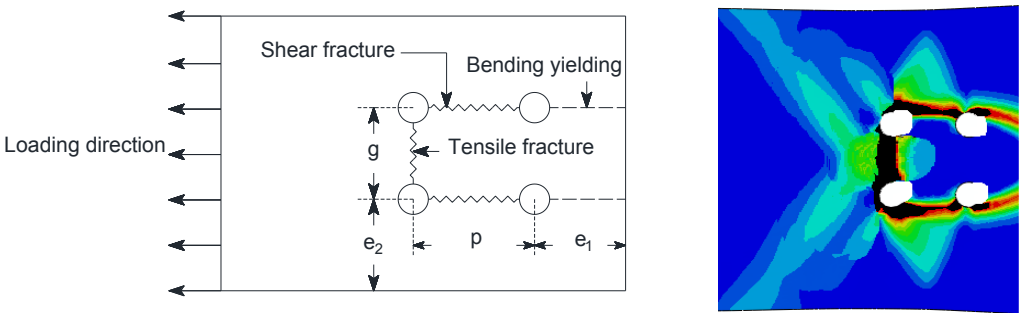

b. Mode 2

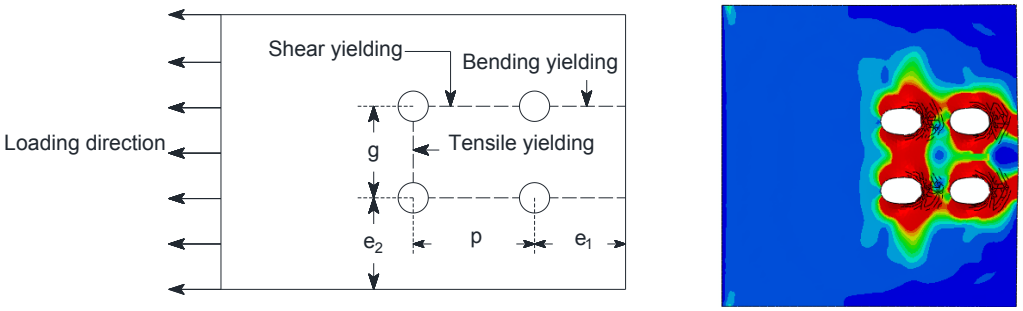

c. Mode 3

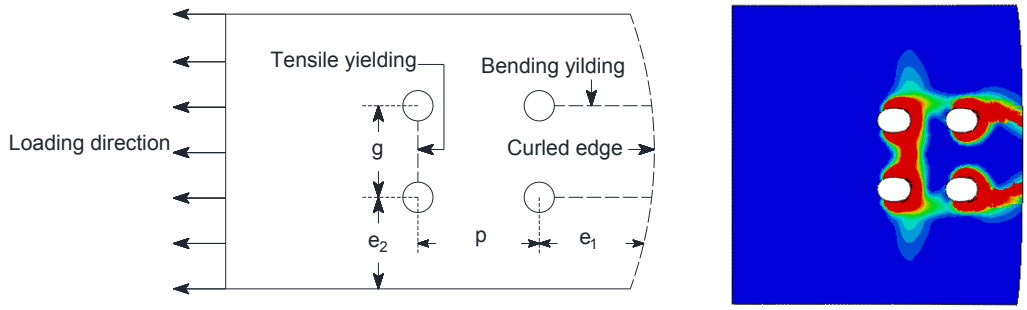

d. Mode 4

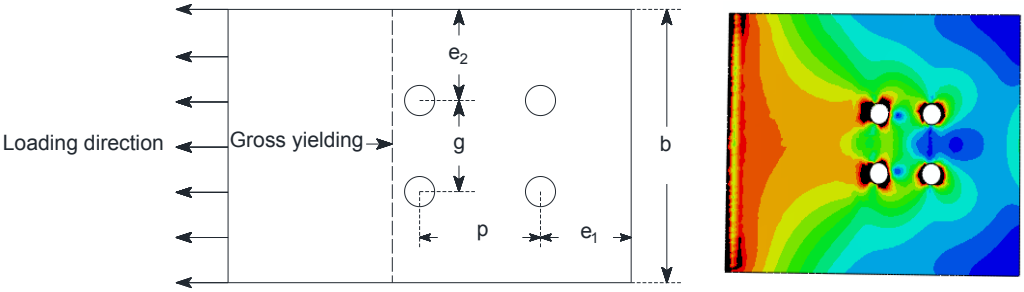

e. Mode 5

Figure 13: Idealized modes of failure

The failure modes for 99 specimens is presented in

Table 5. The analysis of the results reveals the following recommendations for identifying the failure mode to calculate the ultimate strength of single shear bolted connections in thin-walled carbon steel using the previously defined equations.

Mode 1 $e_1 < 18mm$

Mode 2 $18mm \leq e_1 < 24mm$

Mode 3 $24mm \leq e_1 < 30mm$

Mode 4 $30mm \leq e_1 < 42mm\,, for\ t \leq 4mm$ **curling mode**

Mode 4 $30mm \leq e_1 < 48mm\,, for\ t > 4mm$ **curling mode**

Mode 5 $42mm \leq e_1\,, for\ t \leq 4mm$

Mode 5 $48mm \leq e_1\,, for\ t > 4mm$

Comparisons between the ultimate strength calculated by the proposed models ($P_{u\,P}$) and the design standards with the experimental ultimate strength of specimens reported by Kim et al. [10] are presented in Table 6. The comparisons show that the most accurate estimation to the ultimate strength can be obtained using the proposed models. The accuracy of the proposed models is also checked against the FE results and presented in Table 7. The comparison shows that the proposed models can accurately predict the connection strength. However, the proposed models are valid within the range of the investigated parameters: e_1 from 18mm to 60mm, plate thickness from 1.5mm to 6.5mm, e2 equals 60mm, g and p equal 36mm. Therefore, there is a need for further experimental and numerical investigations to validate the proposed equations.

Table 5: Failure modes

Specimen	Failure mode	Specimen	Failure mode	Specimen	Failure mode
T1.5E12	Mode 1	T3.0E48	Mode 5	T5.0E30	Mode 4
T1.5E18	Mode 2	T3.0E54	Mode 5	T5.0E36	Mode 4
T1.5E24	Mode 3	T3.0E60	Mode 5	T5.0E42	Mode 4
T1.5E30	Mode 4	T3.5E12	Mode 1	T5.0E48	Mode 5
T1.5E36	Mode 4	T3.5E18	Mode 2	T5.0E54	Mode 5
T1.5E42	Mode 5	T3.5E24	Mode 3	T5.0E60	Mode 5
T1.5E48	Mode 5	T3.5E30	Mode 4	T5.5E12	Mode 1
T1.5E54	Mode 5	T3.5E36	Mode 4	T5.5E18	Mode 2
T1.5E60	Mode 5	T3.5E42	Mode 5	T5.5E24	Mode 3
T2.0E12	Mode 1	T3.5E48	Mode 5	T5.5E30	Mode 4
T2.0E18	Mode 2	T3.5E54	Mode 5	T5.5E36	Mode 4
T2.0E24	Mode 3	T3.5E60	Mode 5	T5.5E42	Mode 4
T2.0E30	Mode 4	T4.0E12	Mode 1	T5.5E48	Mode 5
T2.0E36	Mode 4	T4.0E18	Mode 2	T5.5E54	Mode 5
T2.0E42	Mode 5	T4.0E24	Mode 3	T5.5E60	Mode 5
T2.0E48	Mode 5	T4.0E30	Mode 4	T6.0E12	Mode 1

T2.0E54	Mode 5	T4.0E36	Mode 4	T6.0E18	Mode 2
T2.0E60	Mode 5	T4.0E42	Mode 4	T6.0E24	Mode 3
T2.5E12	Mode 1	T4.0E48	Mode 5	T6.0E30	Mode 4
T2.5E18	Mode 2	T4.0E54	Mode 5	T6.0E36	Mode 4
T2.5E24	Mode 3	T4.0E60	Mode 5	T6.0E42	Mode 4
T2.5E30	Mode 4	T4.5E12	Mode 1	T6.0E48	Mode 5
T2.5E36	Mode 4	T4.5E18	Mode 2	T6.0E54	Mode 5
T2.5E42	Mode 5	T4.5E24	Mode 3	T6.0E60	Mode 5
T2.5E48	Mode 5	T4.5E30	Mode 4	T6.5E12	Mode 1
T2.5E54	Mode 5	T4.5E36	Mode 4	T6.5E18	Mode 2
T2.5E60	Mode 5	T4.5E42	Mode 4	T6.5E24	Mode 3
T3.0E12	Mode 1	T4.5E48	Mode 5	T6.5E30	Mode 4
T3.0E18	Mode 2	T4.5E54	Mode 5	T6.5E36	Mode 4
T3.0E24	Mode 3	T4.5E60	Mode 5	T6.5E42	Mode 4
T3.0E30	Mode 4	T5.0E12	Mode 1	T6.5E48	Mode 5
T3.0E36	Mode 4	T5.0E18	Mode 2	T6.5E54	Mode 5
T3.0E42	Mode 5	T5.0E24	Mode 3	T6.5E60	Mode 5

Table 6: Ultimate strength of experimental [10], proposed models and design standards

Specimens	**Exp. [10]**	**Proposed**		**EC3**		**AISC and AISI**			
	$P_{u\ exp.}$ kN	$P_{u\ P}$ kN	$P_{u\ exp.}/P_{u\ P}$	$P_{u\ (1)}$ kN Eq.(1)	$P_{u\ exp.}/P_{u\ (1)}$	$P_{u\ (2)}$ kN Eq.(2)	$P_{u\ exp.}/P_{u\ (2)}$	$P_{u\ (3)}$ kN Eq.(3)	$P_{u\ exp.}/P_{u\ (3)}$
T1.5E12	54.68	59.20	0.92	31.95	1.71	48.72	1.12	37.24	1.47
T1.5E18	60.50	65.05	0.93	35.53	1.70	52.43	1.15	41.92	1.44
T1.5E24	61.28	69.70	0.88	39.10	1.57	56.15	1.09	46.61	1.31
T1.5E36	66.12	75.90	0.87	46.25	1.43	63.58	1.04	55.99	1.18
T3.0E24	131.38	139.81	0.94	82.76	1.59	116.96	1.12	106.97	1.23
T3.0E30	134.52	144.88	0.93	89.93	1.50	124.41	1.08	117.73	1.14
T3.0E36	142.92	152.25	0.94	97.11	1.47	131.86	1.08	128.48	1.11
T3.0E48	148.63	161.46	0.92	111.45	1.33	146.76	1.01	150.00	0.99
T3.0E60	153.57	161.46	0.95	125.79	1.22	161.67	0.95	171.51	0.90
T6.0E36	201.00	195.94	1.03	126.84	1.58	171.57	1.17	172.34	1.17
T6.0E48	215.54	207.79	1.04	145.30	1.48	190.75	1.13	201.20	1.07
T6.0E54	220.50	207.79	1.06	154.53	1.43	200.34	1.10	215.63	1.02
T6.0E60	222.40	207.79	1.07	163.75	1.36	209.93	1.06	230.06	0.97

Table 7: Ultimate strength of FE analysis and proposed models

Specimen	Failure mode	$P_{u\,FE}$ (kN)	$P_{n\,P}$ (kN)	$P_{u\,FE}/P_{u\,P}$	EC3		AISC and AISI				Teh et al. [22]	
					P_{u1} (kN) Eq.1	$P_{u\,FE}/P_{u1}$	P_{u2} kN Eq. (2)	$P_{u\,exp.}/P_{u2}$	P_{u3} kN Eq. (3)	$P_{u\,exp.}/P_{u3}$	P_{u4} (kN) Eq.4	$P_{u\,FE}/P_{u4}$
T1.5E12	Mode 1	62.582	65.621	0.954	31.954	0.511	48.719	0.778	37.237	0.595	44.703	0.714
T1.5E18	Mode 2	67.525	67.397	1.002	35.529	0.526	52.435	0.777	41.924	0.621	53.449	0.792
T1.5E24	Mode 3	69.087	71.827	0.962	39.104	0.566	56.150	0.813	46.612	0.675	57.164	0.827
T1.5E30	Mode 4	71.622	74.304	0.964	42.679	0.596	59.865	0.836	51.299	0.716	60.879	0.850
T1.5E36	Mode 4	73.102	78.019	0.937	46.254	0.633	63.580	0.870	55.986	0.766	64.594	0.884
T1.5E42	Mode 5	77.121	80.496	0.958	49.829	0.646	67.295	0.873	60.673	0.787	68.310	0.886
T1.5E48	Mode 5	77.542	80.496	0.963	53.404	0.689	71.011	0.916	65.360	0.843	72.025	0.929
T1.5E54	Mode 5	77.769	80.496	0.966	56.979	0.733	74.726	0.961	70.048	0.901	75.740	0.974
T1.5E60	Mode 5	77.917	80.496	0.968	60.554	0.777	78.441	1.007	74.735	0.959	79.455	1.020
T2.0E12	Mode 1	88.103	87.494	1.007	42.605	0.484	64.959	0.737	49.650	0.564	66.311	0.753
T2.0E18	Mode 2	88.462	89.862	0.984	47.372	0.536	69.913	0.790	55.899	0.632	71.265	0.806
T2.0E24	Mode 3	90.893	95.770	0.949	52.139	0.574	74.866	0.824	62.149	0.684	76.219	0.839
T2.0E30	Mode 4	92.561	99.072	0.934	56.905	0.615	79.820	0.862	68.398	0.739	81.172	0.877
T2.0E36	Mode 4	98.987	104.026	0.952	61.672	0.623	84.774	0.856	74.648	0.754	86.126	0.870
T2.0E42	Mode 5	103.124	107.328	0.961	66.438	0.644	89.727	0.870	80.898	0.784	91.079	0.883
T2.0E48	Mode 5	103.465	107.328	0.964	71.205	0.688	94.681	0.915	87.147	0.842	96.033	0.928
T2.0E54	Mode 5	103.566	107.328	0.965	75.972	0.734	99.634	0.962	93.397	0.902	100.987	0.975
T2.0E60	Mode 5	103.723	107.328	0.966	80.738	0.778	104.588	1.008	99.646	0.961	105.940	1.021
T2.5E12	Mode 1	105.931	109.368	0.969	53.257	0.503	81.199	0.767	62.062	0.586	82.889	0.782
T2.5E18	Mode 2	109.704	112.328	0.977	59.215	0.540	87.391	0.797	69.874	0.637	89.081	0.812
T2.5E24	Mode 3	114.627	119.712	0.958	65.173	0.569	93.583	0.816	77.686	0.678	95.273	0.831
T2.5E30	Mode 4	119.359	123.840	0.964	71.131	0.596	99.775	0.836	85.498	0.716	101.465	0.850

Specimen	Failure mode	$P_{u\,FE}$ (kN)	$P_{n\,P}$ (kN)	$P_{u\,FE}/P_{u\,P}$	EC3		AISC and AISI				Teh et al. [22]	
					P_{u1} (kN) Eq.1	$P_{u\,FE}/P_{u1}$	P_{u2} kN Eq. (2)	$P_{u\,exp.}/P_{u2}$	P_{u3} kN Eq. (3)	$P_{u\,exp.}/P_{u3}$	P_{u4} (kN) Eq.4	$P_{u\,FE}/P_{u4}$
T2.5E36	Mode 4	123.767	130.032	0.952	77.090	0.623	105.967	0.856	93.310	0.754	107.657	0.870
T2.5E42	Mode 5	130.418	134.160	0.972	83.048	0.637	112.159	0.860	101.122	0.775	113.849	0.873
T2.5E48	Mode 5	131.275	134.160	0.978	89.006	0.678	118.351	0.902	108.934	0.830	120.041	0.914
T2.5E54	Mode 5	132.502	134.160	0.988	94.964	0.717	124.543	0.940	116.746	0.881	126.233	0.953
T2.5E60	Mode 5	133.012	134.160	0.991	100.923	0.759	130.735	0.983	124.558	0.936	132.425	0.996
T3.0E12	Mode 1	133.678	131.242	1.019	63.908	0.478	97.439	0.729	74.474	0.557	99.467	0.744
T3.0E18	Mode 2	133.839	134.794	0.993	71.058	0.531	104.869	0.784	83.849	0.626	106.898	0.799
T3.0E24	Mode 3	138.666	143.654	0.965	78.208	0.564	112.300	0.810	93.223	0.672	114.328	0.824
T3.0E30	Mode 4	143.625	148.608	0.966	85.358	0.594	119.730	0.834	102.598	0.714	121.758	0.848
T3.0E36	Mode 4	152.014	156.038	0.974	92.508	0.609	127.160	0.837	111.972	0.737	129.189	0.850
T3.0E42	Mode 5	155.325	160.992	0.965	99.658	0.642	134.591	0.867	121.346	0.781	136.619	0.880
T3.0E48	Mode 5	155.655	156.780	0.993	106.807	0.686	142.021	0.912	130.721	0.840	144.050	0.925
T3.0E54	Mode 5	155.931	156.780	0.995	113.957	0.731	149.452	0.958	140.095	0.898	151.480	0.971
T3.0E60	Mode 5	156.142	156.780	0.996	121.107	0.776	156.882	1.005	149.470	0.957	158.910	1.018
T3.5E12	Mode 1	150.663	153.115	0.984	74.559	0.495	113.679	0.755	86.887	0.577	116.045	0.770
T3.5E18	Mode 2	156.717	155.243	1.009	82.901	0.529	122.347	0.781	97.824	0.624	124.714	0.796
T3.5E24	Mode 3	161.478	167.597	0.963	91.243	0.565	131.016	0.811	108.760	0.674	133.383	0.826
T3.5E30	Mode 4	164.612	173.376	0.949	99.584	0.605	139.685	0.849	119.697	0.727	142.051	0.863
T3.5E36	Mode 4	171.630	182.045	0.943	107.926	0.629	148.354	0.864	130.634	0.761	150.720	0.878
T3.5E42	Mode 5	182.592	187.824	0.972	116.267	0.637	157.023	0.860	141.571	0.775	159.389	0.873
T3.5E48	Mode 5	182.503	187.824	0.972	124.609	0.683	165.691	0.908	152.508	0.836	168.058	0.921
T3.5E54	Mode 5	182.487	187.824	0.972	132.950	0.729	174.360	0.955	163.444	0.896	176.727	0.968
T3.5E60	Mode 5	183.517	187.824	0.977	141.292	0.770	183.029	0.997	174.381	0.950	185.395	1.010
T4.0E12	Mode 1	178.056	174.989	1.018	85.211	0.479	129.918	0.730	99.299	0.558	132.623	0.745
T4.0E18	Mode 2	178.154	177.165	1.006	94.744	0.532	139.826	0.785	111.798	0.628	142.530	0.800
T4.0E24	Mode 3	185.421	191.539	0.968	104.277	0.562	149.733	0.808	124.298	0.670	152.437	0.822
T4.0E30	Mode 4	189.222	198.144	0.955	113.810	0.601	159.640	0.844	136.797	0.723	162.345	0.858
T4.0E36	Mode 4	198.954	208.051	0.956	123.344	0.620	169.547	0.852	149.296	0.750	172.252	0.866
T4.0E42	Mode 4	212.106	220.160	0.963	132.877	0.626	179.454	0.846	161.795	0.763	182.159	0.859
T4.0E48	Mode 5	208.235	214.656	0.970	142.410	0.684	189.362	0.909	174.294	0.837	192.066	0.922
T4.0E54	Mode 5	208.468	214.656	0.971	151.943	0.729	199.269	0.956	186.794	0.896	201.973	0.969
T4.0E60	Mode 5	208.956	214.656	0.973	161.476	0.773	209.176	1.001	199.293	0.954	211.881	1.014
T4.5E12	Mode 1	194.538	196.862	0.988	95.862	0.493	146.158	0.751	111.712	0.574	149.201	0.767
T4.5E18	Mode 2	201.736	202.190	0.998	106.587	0.528	157.304	0.780	125.773	0.623	160.346	0.795
T4.5E24	Mode 3	208.172	215.482	0.966	117.312	0.564	168.449	0.809	139.835	0.672	171.492	0.824
T4.5E30	Mode 4	215.723	222.912	0.968	128.037	0.594	179.595	0.833	153.896	0.713	182.638	0.847
T4.5E36	Mode 4	222.354	234.058	0.950	138.762	0.624	190.741	0.858	167.958	0.755	193.783	0.872
T4.5E42	Mode 4	230.789	247.680	0.932	149.486	0.648	201.886	0.875	182.020	0.789	204.929	0.888
T4.5E48	Mode 5	239.906	241.488	0.993	160.211	0.668	213.032	0.888	196.081	0.817	216.074	0.901
T4.5E54	Mode 5	240.059	241.488	0.994	170.936	0.712	224.177	0.934	210.143	0.875	227.220	0.947
T4.5E60	Mode 5	241.308	241.488	0.999	181.661	0.753	235.323	0.975	224.204	0.929	238.366	0.988
T5.0E12	Mode 1	222.351	218.736	1.017	106.513	0.479	162.398	0.730	124.124	0.558	165.779	0.746
T5.0E18	Mode 2	223.964	224.656	0.997	118.430	0.529	174.782	0.780	139.748	0.624	178.163	0.795
T5.0E24	Mode 3	231.582	239.424	0.967	130.346	0.563	187.166	0.808	155.372	0.671	190.547	0.823
T5.0E30	Mode 4	238.687	247.680	0.964	142.263	0.596	199.550	0.836	170.996	0.716	202.931	0.850
T5.0E36	Mode 4	248.729	260.064	0.956	154.179	0.620	211.934	0.852	186.620	0.750	215.315	0.866
T5.0E42	Mode 4	257.798	275.200	0.937	166.096	0.644	224.318	0.870	202.244	0.785	227.699	0.883
T5.0E48	Mode 5	260.243	268.320	0.970	178.012	0.684	236.702	0.910	217.868	0.837	240.083	0.923
T5.0E54	Mode 5	260.685	268.320	0.972	189.929	0.729	249.086	0.956	233.492	0.896	252.467	0.968
T5.0E60	Mode 5	261.015	268.320	0.973	201.845	0.773	261.470	1.002	249.116	0.954	264.851	1.015
T5.5E12	Mode 1	240.525	240.610	1.000	117.165	0.487	178.638	0.743	136.536	0.568	182.357	0.758
T5.5E18	Mode 2	249.299	247.122	1.009	130.273	0.523	192.260	0.771	153.723	0.617	195.979	0.786
T5.5E24	Mode 3	255.706	263.366	0.971	143.381	0.561	205.883	0.805	170.909	0.668	209.601	0.820
T5.5E30	Mode 4	261.189	272.448	0.959	156.489	0.599	219.505	0.840	188.096	0.720	223.224	0.855
T5.5E36	Mode 4	271.051	286.070	0.947	169.597	0.626	233.127	0.860	205.282	0.757	236.846	0.874
T5.5E42	Mode 4	279.629	302.720	0.924	182.706	0.653	246.750	0.882	222.468	0.796	250.469	0.896
T5.5E48	Mode 5	290.128	295.152	0.983	195.814	0.675	260.372	0.897	239.655	0.826	264.091	0.910
T5.5E54	Mode 5	293.291	295.152	0.994	208.922	0.712	273.995	0.934	256.841	0.876	277.713	0.947
T5.5E60	Mode 5	293.713	295.152	0.995	222.030	0.756	287.617	0.979	274.028	0.933	291.336	0.992

Specimen	Failure mode	$P_{u\,FE}$ (kN)	$P_{n\,P}$ (kN)	$P_{u\,FE}/P_{u\,P}$	EC3		AISC and AISI				Teh et al. [22]	
					P_{u1} (kN) Eq.1	$P_{u\,FE}/P_{u1}$	P_{u2} kN Eq. (2)	$P_{u\,exp.}/P_{u2}$	P_{u3} kN Eq. (3)	$P_{u\,exp.}/P_{u3}$	P_{u4} (kN) Eq.4	$P_{u\,FE}/P_{u4}$
T6.0E12	Mode 1	266.351	262.483	1.015	127.816	0.480	194.878	0.732	148.949	0.559	198.934	0.747
T6.0E18	Mode 2	267.569	269.587	0.993	142.116	0.531	209.738	0.784	167.698	0.627	213.795	0.799
T6.0E24	Mode 3	275.842	287.309	0.960	156.416	0.567	224.599	0.814	186.446	0.676	228.656	0.829
T6.0E30	Mode 4	285.876	297.216	0.962	170.716	0.597	239.460	0.838	205.195	0.718	243.517	0.852
T6.0E36	Mode 4	298.658	312.077	0.957	185.015	0.619	254.321	0.852	223.944	0.750	258.378	0.865
T6.0E42	Mode 4	315.586	330.240	0.956	199.315	0.632	269.182	0.853	242.693	0.769	273.238	0.866
T6.0E48	Mode 5	314.651	321.984	0.977	213.615	0.679	284.042	0.903	261.442	0.831	288.099	0.916
T6.0E54	Mode 5	314.782	321.984	0.978	227.915	0.724	298.903	0.950	280.190	0.890	302.960	0.962
T6.0E60	Mode 5	314.928	321.984	0.978	242.215	0.769	313.764	0.996	298.939	0.949	317.821	1.009
T6.5E12	Mode 1	280.291	284.357	0.986	138.467	0.494	211.117	0.753	161.361	0.576	215.512	0.769
T6.5E18	Mode 2	291.683	292.053	0.999	153.959	0.528	227.217	0.779	181.672	0.623	231.611	0.794
T6.5E24	Mode 3	303.239	311.251	0.974	169.450	0.559	243.316	0.802	201.984	0.666	247.711	0.817
T6.5E30	Mode 4	313.737	321.984	0.974	184.942	0.589	259.415	0.827	222.295	0.709	263.810	0.841
T6.5E36	Mode 4	324.402	338.083	0.960	200.433	0.618	275.514	0.849	242.606	0.748	279.909	0.863
T6.5E42	Mode 4	333.942	357.760	0.933	215.925	0.647	291.613	0.873	262.917	0.787	296.008	0.886
T6.5E48	Mode 5	341.808	348.816	0.980	231.416	0.677	307.713	0.900	283.228	0.829	312.107	0.913
T6.5E54	Mode 5	346.094	348.816	0.992	246.908	0.713	323.812	0.936	303.540	0.877	328.207	0.948
T6.5E60	Mode 5	348.047	348.816	0.998	262.399	0.754	339.911	0.977	323.851	0.930	344.306	0.989
Mean				0.97		0.62		0.86		0.75		0.87
Standard deviation				0.02		0.09		0.08		0.12		0.08
Coefficient of variation				0.02		0.14		0.09		0.15		0.09

6. SUMMARY AND CONCLUSIONS

The ultimate strength and the failure sequence of bolted single-shear connections in thin-walled carbon steel was investigated using finite element analysis. Parametric study was performed to evaluate the effect of the influential parameters on the connection behaviour. The output of the finite element analysis was used to propose analytical models to estimate the ultimate strength of the connections. The proposed models are based on three failure criteria: tensile, shear and bending along the end distance in addition to the curling. The models were validated against experimental [10] data and they provided excellent prediction of the connection ultimate strength. The design standards for steel structures such as EC3, AISI and AISC tend to underestimate the connection strength comparing with the experimental data [10]. However, the proposed models provide more accurate estimation of the connection strength. The strain distribution of the steel plate was investigated and revealed five failure modes. It is recommended to limit the maximum end distance to 50mm as no strength improvement can be obtained beyond this limit. The curling displacement affects the patterns of yielding and controls the connection strength and is considered as sign of failure only when it reaches 0.5mm before the ultimate strength of the connection is reached. The existence of curling could reduce the connection strength by 12% and results in sharper drop in the strength after the ultimate strength.

REFERENCES

1. Kulak, G.L., J.W. Fisher, and J.H. Struik, *Guide to Design Criteria for Bolted and Riveted Joints Second Edition.* 2001.
2. Winter, G., *Tests on bolted connections in light gage steel.* Journal of the Structural Division, 1956. **82**(2): p. 1-25.
3. Kim, H.J. and J.A. Yura, *The effect of ultimate-to-yield ratio on the bearing strength of bolted connections.* Journal of Constructional Steel Research, 1999. **49**(3): p. 255-269.
4. Topkaya, C., *A finite element parametric study on block shear failure of steel tension members.* Journal of Constructional Steel Research, 2004. **60**(11): p. 1615-1635.
5. Kim and Kuwamura, *Finite Element Modeling of Bolted Connections in Thin-Walled Stainless Steel Plates under Static Shear.* Thin-Walled Structures, 2007. **45**(4): p. 407-421.
6. Kim, T.S., H. Kuwamura, and T.J. Cho, *A Parametric Study on Ultimate Strength of Single Shear Bolted Connections with Curling.* Thin-Walled Structures, 2008. **46**(1): p. 38-53.
7. Teh, L.H. and D.D.A. Clements, *Block Shear Capacity of Bolted Connections in Cold-Reduced Steel Sheets.* Journal of Structural Engineering, 2012. **138**(4): p. 459-467.
8. Clements, D.D.A. and L.H. Teh, *Active Shear Planes of Bolted Connections Failing in Block Shear.* Journal of Structural Engineering, 2013. **139**(3): p. 320-327.
9. Kim, T. and J. Lim, *Ultimate strength of single shear two-bolted connections with austenitic stainless steel.* International Journal of Steel Structures, 2013. **13**(1): p. 117-128.
10. Kim, T., J. Yoo, and C.W. Roeder, *Experimental Investigation on Strength and Curling Influence of Bolted Connections in Thin-Walled Carbon Steel.* Thin-Walled Structures, 2015. **91**(Supplement C): p. 1-12.
11. Kim, T., M. Kim, and T. Cho, *Parametric Study on Ultimate Strength of Four-bolted Connections with Cold-formed Carbon Steel.* International Journal of Steel Structures, 2018. **18**(1): p. 265-280.
12. Repair, H. *Flowdrill*. 2019 2019]]; Available from: http://m.help-repair.info/construction_and_infrastructure/light_steel_thinwalled_structures_lstc.
13. Dassault, *Abaqus v. 6.13-2 [Software]*, in *Dassault Systèmes Simulia Corp*. 2013, Providence, RI: Dassault Systèmes Simulia Corp.
14. Chung, K.F. and K.H. Ip, *Finite element modeling of bolted connections between cold-formed steel strips and hot rolled steel plates under static shear loading.* Engineering Structures, 2000. **22**(10): p. 1271-1284.
15. Mahmood, M., W. Tizani, and C. Sansour, *Effect of Tube Thickness on the Face Bending for Blind-Bolted Connection to Concrete Filled Tubular Structures.* International Journal of Civil, Architectural, Structural and Construction Engineering, 2014. **8**(9): p. 904-910.
16. Epstein, H.I. and M.J. McGinnis, *Finite element modeling of block shear in structural tees.* Computers & Structures, 2000. **77**(5): p. 571-582.
17. Kim, T.S. and H. Kuwamura, *Numerical Investigation on Strength Design and Curling Effect of Mechanically Fastened Joints In Cold-Formed Austenitic Stainless Steel.* Materials & Design, 2011. **32**(7): p. 3942-3956.
18. Lecce, M. and K.J.R. Rasmussen, *Nonlinear Flange Curling in Wide Flange Sections.* Journal of Constructional Steel Research, 2008. **64**(7): p. 779-784.
19. CEN, *Eurocode 3: Design of steel structures - Part 1-3-General Rules: Supplementary rules for cold formed thin gauge members and sheeting.*, in *EN 1996-1-3*. 2005, CEN.
20. CEN, *Eurocode 3: Design of steel structures - Part 1-8: Design of joints*, in *EN 1993-1-8*. 2005, CEN.
21. (AISI), *North American specification for the design of cold-formed steel structural members*, in *AISI S100-12*. 2012, American Iron and Steel Institute: Washington D.C.,USA.
22. (AISC), *Steel construction manual*. 2011, American Institute of Steel Construction: USA.
23. Teh, L.H. and D. Clements, *Block Shear Capacity of Bolted Connections in Cold-Reduced Steel Sheets.* Journal of Structural Engineering, ASCE, 2011. **138**(4): p. 459-467.